

## Locus coeruleus imaging as a biomarker for noradrenergic dysfunction in neurodegenerative diseases

Matthew J. Betts,<sup>1,2</sup> Evgeniya Kirilina,<sup>3,4</sup> Maria C.G. Otaduy,<sup>5</sup> Dimo Ivanov,<sup>6</sup> Julio Acosta-Cabronero,<sup>7</sup> Martina F. Callaghan,<sup>7</sup> Christian Lambert,<sup>7</sup> Arturo Cardenas-Blanco,<sup>1,2</sup> Kerrin Pine,<sup>3,7</sup> Luca Passamonti,<sup>8,9</sup> Clare Loane,<sup>10</sup> Max C. Keuken,<sup>11,12</sup> Paula Trujillo,<sup>13</sup> Falk Lüsebrink,<sup>14,15</sup> Hendrik Mattern,<sup>14</sup> Kathy Y. Liu,<sup>16</sup> Nikos Priovoulos,<sup>17</sup> Klaus Fliessbach,<sup>18,19</sup> Martin J. Dahl,<sup>20</sup> Anne Maaß,<sup>1</sup> Christopher F. Madelung,<sup>21</sup> David Meder,<sup>21</sup> Alexander J. Ehrenberg,<sup>22,23</sup> Oliver Speck,<sup>1,14,24,25</sup> Nikolaus Weiskopf,<sup>3,7</sup> Raymond Dolan,<sup>7,26</sup> Ben Inglis,<sup>27</sup> Duygu Tosun,<sup>28</sup> Markus Morawski,<sup>29</sup> Fabio A. Zucca,<sup>30</sup> Hartwig R. Siebner,<sup>21</sup> Mara Mather,<sup>31</sup> Kamil Uludag,<sup>32,33</sup> Helmut Heinsen,<sup>34,35</sup> Benedikt A. Poser,<sup>6</sup> Robert Howard,<sup>16</sup> Luigi Zecca,<sup>30,36</sup> James B. Rowe,<sup>8</sup> Lea T. Grinberg,<sup>22,34,37</sup> Heidi I.L. Jacobs,<sup>6,38,39</sup> Emrah Düzel<sup>1,2,10,\*</sup> and Dorothea Hämmerer<sup>2,7,10,\*</sup>

\*These authors contributed equally to this work.

Pathological alterations to the locus coeruleus, the major source of noradrenaline in the brain, are histologically evident in early stages of neurodegenerative diseases. Novel MRI approaches now provide an opportunity to quantify structural features of the locus coeruleus *in vivo* during disease progression. In combination with neuropathological biomarkers, *in vivo* locus coeruleus imaging could help to understand the contribution of locus coeruleus neurodegeneration to clinical and pathological manifestations in Alzheimer's disease, atypical neurodegenerative dementias and Parkinson's disease. Moreover, as the functional sensitivity of the noradrenergic system is likely to change with disease progression, *in vivo* measures of locus coeruleus integrity could provide new pathophysiological insights into cognitive and behavioural symptoms. Locus coeruleus imaging also holds the promise to stratify patients into clinical trials according to noradrenergic dysfunction. In this article, we present a consensus on how non-invasive *in vivo* assessment of locus coeruleus integrity can be used for clinical research in neurodegenerative diseases. We outline the next steps for *in vivo*, post-mortem and clinical studies that can lay the groundwork to evaluate the potential of locus coeruleus imaging as a biomarker for neurodegenerative diseases.

- 1 German Center for Neurodegenerative Diseases (DZNE), Magdeburg, Germany
- 2 Institute of Cognitive Neurology and Dementia Research, Otto-von-Guericke-University Magdeburg, Magdeburg, Germany
- 3 Department of Neurophysics, Max Planck Institute for Human Cognitive and Brain Sciences, Leipzig, Germany
- 4 Center for Cognitive Neuroscience, Free University Berlin, Berlin, Germany
- 5 Laboratory of Magnetic Resonance LIM44, Department and Institute of Radiology, Medical School of the University of São Paulo, Brazil
- 6 Department of Cognitive Neuroscience, Faculty of Psychology and Neuroscience, Maastricht University, 6200 MD, Maastricht, Netherlands
- 7 Wellcome Centre for Human Neuroimaging, UCL Institute of Neurology, London, UK
- 8 Department of Clinical Neurosciences, University of Cambridge, UK
- 9 Consiglio Nazionale delle Ricerche, Istituto di Bioimmagini e Fisiologia Molecolare (IBFM), Milan, Italy
- 10 Institute of Cognitive Neuroscience, University College London, London, UK

Received February 22, 2019. Revised April 12, 2019. Accepted May 1, 2019

© The Author(s) (2019). Published by Oxford University Press on behalf of the Guarantors of Brain.

This is an Open Access article distributed under the terms of the Creative Commons Attribution Non-Commercial License (<http://creativecommons.org/licenses/by-nc/4.0/>), which permits non-commercial re-use, distribution, and reproduction in any medium, provided the original work is properly cited. For commercial re-use, please contact [journals.permissions@oup.com](mailto:journals.permissions@oup.com)

- 11 University of Amsterdam, Integrative Model-based Cognitive Neuroscience research unit, Amsterdam, The Netherlands
- 12 University of Leiden, Cognitive Psychology, Leiden, The Netherlands
- 13 Department of Neurology, Vanderbilt University Medical Center, Nashville, TN, USA
- 14 Department of Biomedical Magnetic Resonance, Institute for Physics, Otto-von-Guericke-University, Magdeburg, Germany
- 15 Department of Neurology, Otto-von-Guericke University, Magdeburg, Germany
- 16 Division of Psychiatry, University College London, London, UK
- 17 Faculty of Health, Medicine and Life Sciences, School for Mental Health and Neuroscience, Alzheimer Centre Limburg, Maastricht University, Maastricht, The Netherlands
- 18 Department for Neurodegenerative Diseases and Geriatric Psychiatry, University Hospital Bonn, Bonn, Germany
- 19 German Center for Neurodegenerative Diseases (DZNE), Bonn, Germany
- 20 Center for Lifespan Psychology, Max Planck Institute for Human Development, Berlin, Germany
- 21 Danish Research Centre for Magnetic Resonance, Centre for Functional and Diagnostic Imaging and Research, Copenhagen University Hospital Hvidovre, Denmark
- 22 Memory and Aging Center, Weill Institute for Neurosciences, University of California, San Francisco, San Francisco, CA, USA
- 23 Department of Integrative Biology, University of California, Berkeley, Berkeley, CA, USA
- 24 Center for Behavioral Brain Sciences, Magdeburg, Germany
- 25 Leibniz Institute for Neurobiology, Magdeburg, Germany
- 26 Max Planck Centre for Computational Psychiatry and Ageing, University College London, UK
- 27 Henry H. Wheeler, Jr. Brain Imaging Center, University of California, Berkeley, CA, USA
- 28 Department of Radiology and Biomedical Imaging, University of California - San Francisco, San Francisco, CA, USA
- 29 Paul Flechsing Institute of Brain Research, Medical Faculty, University of Leipzig, Leipzig, Germany
- 30 Institute of Biomedical Technologies, National Research Council of Italy, Segrate, Milan, Italy
- 31 Leonard Davis School of Gerontology and Department of Psychology, University of Southern California, Los Angeles, CA, USA
- 32 Centre for Neuroscience Imaging Research, Institute for Basic Science and Department of Biomedical Engineering, Sungkyunkwan University, Suwon, Republic of Korea
- 33 Techna Institute and Koerner Scientist in MR Imaging, University Health Network, Toronto, Canada
- 34 University of São Paulo Medical School, São Paulo, Brazil
- 35 Clinic of Psychiatry, University of Würzburg, Würzburg, Germany
- 36 Department of Psychiatry, Columbia University Medical Center, New York State Psychiatric Institute, New York, USA
- 37 Global Brain Health Institute, University of California, San Francisco, San Francisco, CA, USA
- 38 Division of Nuclear Medicine and Molecular Imaging, Department of Radiology, Massachusetts General Hospital/Harvard Medical School, Boston, MA, USA
- 39 Faculty of Health, Medicine and Life Sciences, School for Mental Health and Neuroscience, Alzheimer Centre Limburg, Maastricht University, Maastricht, The Netherlands

Correspondence to: Matthew J. Betts  
 German Center for Neurodegenerative Diseases (DZNE)  
 Magdeburg, Germany  
 E-mail: matthew.betts@dzne.de

**Keywords:** locus coeruleus (LC); magnetic resonance imaging (MRI); neurodegeneration; noradrenaline (NA), biomarker

**Abbreviations:** LC = locus coeruleus; MT = magnetization transfer

## Introduction

The number of individuals over the age of 60 years is projected to rise from 841 million in 2013 to over 2 billion by 2050 (World Population Ageing report, United Nations). As the population has continued to age, age-related neurodegenerative diseases have already reached epidemic proportions. Whilst numerous therapeutic strategies are being investigated, current treatments provide only modest symptomatic relief and do not slow or halt ensuing neurodegeneration. A major priority is to develop early disease stage biomarkers that can improve the understanding of the pathophysiology of neurodegenerative diseases, enable earlier detection of pathology and facilitate the application of timely symptomatic interventions.

The locus coeruleus (LC) is the major source of noradrenaline modulation in the brain and has been shown to be involved in regulating a wide range of higher cognitive functions, such as working memory, learning and attention (Robbins, 1984; Aston-Jones and Cohen, 2005; Benarroch, 2009; Mather *et al.*, 2016), memory consolidation and retrieval (Sterpenich *et al.*, 2006; Sara, 2009), vigilance, arousal/wakefulness, rapid eye movement (REM) sleep behaviour, pain modulation, local blood flow and immunological mechanisms in the brain (Aston-Jones and Bloom, 1981; Benarroch, 2009; Espay *et al.*, 2014; Heneka *et al.*, 2015; O'Donnell *et al.*, 2015). Conversely, age-related decline within the LC–noradrenergic system is associated with reduced cognitive abilities relating to episodic memory (Hämmerer *et al.*, 2018,

Jacobs *et al.*, 2018*b*; Dahl *et al.*, 2019) and reduced cognitive reserve (Robertson, 2013; Wilson *et al.*, 2013; Clewett *et al.*, 2016; Mather and Harley, 2016). In Alzheimer's disease, tau aggregates are observed first in the LC, prior to their presence in transentorhinal/entorhinal cortex and neocortex (Braak *et al.*, 2011; Stratmann *et al.*, 2016; Andrés-Benito *et al.*, 2017; Ehrenberg *et al.*, 2017). In Parkinson's disease, intraneuronal  $\alpha$ -synuclein burden in the LC precedes and may be of even greater magnitude than that in the dopaminergic substantia nigra pars compacta (SNpc) (Braak *et al.*, 2003; Dickson *et al.*, 2008). As a result, the degree of Parkinson's disease-related neuronal loss is likely just as severe in the LC as in the SNpc (Zarow

*et al.*, 2003; Giguère *et al.*, 2018). Pathological changes in the LC have also been reported in other neurodegenerative and neuropsychiatric conditions (Box 1), leading to the notion that the LC may be a vulnerable target for pathology (Sharma *et al.*, 2010). Whether this is related to LC neurons' high metabolic need in order to maintain essential physiological functions or the close proximity of the LC to the fourth ventricle, exposing it to toxins from the CSF (Mather and Harley, 2016; Weinschenker, 2018), remains to be determined.

With the notable exception of most of the basal ganglia, the LC projects to large portions of subcortical and cortical areas (Berridge and Waterhouse, 2003). Moreover,

### Box 1 Role of the LC in neurological disorders

Structural and functional changes in the human LC leading to deficits in noradrenaline may contribute to the pathophysiology and symptomatology of several neurological disorders:

#### Alzheimer's disease

Deposition of tau in and degeneration of the LC occurs early in the asymptomatic phase of Alzheimer's disease (Braak and Del Tredici, 2012; Arendt *et al.*, 2015) suggesting that the LC is the initial site of pathology. Accumulation of tau (doubling from Braak stage 0 to I; Ehrenberg *et al.*, 2017) and significant volume loss precede neuronal loss in the LC during Alzheimer's disease progression (Theofilas *et al.*, 2017). Depletion of up to 30% of LC neurons has been reported in prodromal (mild cognitive impairment stage) Alzheimer's disease, increasing to 55% with diagnosed dementia (Kelly *et al.*, 2017). Neuronal loss is particularly prevalent in the rostral/middle portion of the LC (German *et al.*, 1992; Theofilas *et al.*, 2017), correlating with cognitive dysfunction including memory, perceptual speed, and visuo-spatial ability (Kelly *et al.*, 2017), and with reduced noradrenaline levels in hippocampus and cortex (Lyness, 2003). Compensatory activity, such as increased metabolism in surviving neurons or reorganization of functional networks, can occur in early disease stages (Hoogendijk *et al.*, 1999; Jacobs *et al.*, 2015).

#### Synucleinopathies

In Parkinson's disease and dementia with Lewy bodies,  $\alpha$ -synuclein containing Lewy bodies and neuronal cell loss are seen along the entire length of the LC (German *et al.*, 1992; Theofilas *et al.*, 2017). Intraneuronal Lewy bodies also affect tyrosine hydroxylase (TH) activity, potentially interfering with normal catecholamine biosynthesis (Tabrez *et al.*, 2012), which may distinguish the effects of Parkinson's disease/dementia with Lewy bodies from Alzheimer's disease (McMillan *et al.*, 2011). It has also been postulated that LC burden precedes substantia nigra involvement in Parkinson's disease (Zarow *et al.*, 2003; Braak *et al.*, 2004; Seidel *et al.*, 2015), rendering the LC a good candidate for preclinical diagnosis (Liu *et al.*, 2017). However, the field lacks a comprehensive analysis detailing the stages of neuronal loss in Parkinson's disease.

Multiple system atrophy (MSA) is another heterogeneous  $\alpha$ -synucleinopathy, in which autonomic dysfunction, parkinsonism, and ataxia (Stankovic *et al.*, 2014; Walsh *et al.*, 2018) are associated with severe neuronal loss in the LC and noradrenergic cardiorespiratory brainstem nuclei (A5, A1) (Benarroch *et al.*, 2008). An *in vivo* neuromelanin-sensitive MRI study has shown that LC contrast is reduced in MSA compared to healthy controls and that the ratio of neuromelanin-sensitive MRI contrast in substantia nigra versus LC could help distinguish MSA from Parkinson's disease (Matsuura *et al.*, 2013).

Patients with idiopathic rapid eye movement sleep disorder (iRBD) have a strongly increased risk of developing Parkinson's disease, dementia with Lewy bodies, MSA and mild cognitive impairment; 75.7% and 90.9% develop a neurodegenerative syndrome 10 and 14 years from the time of iRBD diagnosis, respectively. Interestingly, iRBD is associated with dysfunction of the LC-noradrenergic system (Knudsen *et al.*, 2018) suggesting that LC imaging might serve as a valuable biomarker in patients at risk of developing neurodegenerative disease.

#### Chronic traumatic encephalopathy

In addition to early pathological affection of cortical sulci, substantial LC damage and tau accumulation has also been reported in early disease stages (Stein *et al.*, 2014). LC pathology may also exacerbate clinical presentation of cognitive complaints and mood disturbances in chronic traumatic encephalopathy (Stern and Daneshvar, 2013).

#### Frontotemporal lobar degeneration

Modest LC neuronal loss occurs in both tau- and non-tau- forms of frontotemporal lobar degeneration (Brunnström *et al.*, 2011; Eser *et al.*, 2018), both in early and late disease stages (Irwin *et al.*, 2016). Clinically, the loss and dysregulation of noradrenaline from LC degeneration may contribute to cognitive decline, including impulsivity and apathy (Passamonti *et al.*, 2018).

#### Essential tremor

A neuropathological study ( $n = 33$ ) revealed Lewy body pathology in the LC in 25% of the cases with essential tremor (Louis *et al.*, 2007). Noradrenergic LC-cerebellar connections are important for the normal function of Purkinje cells and their inhibitory output (Moises *et al.*, 1981). Degeneration and ensuing LC dysfunction may modulate Purkinje cell activity and contribute to decreased cerebellar inhibition in essential tremor (Louis *et al.*, 2007).

#### Non-degenerative, neuropsychiatric illnesses

LC dysfunction, also without neuronal loss, has also been implicated in post-traumatic stress disorder (Bernard *et al.*, 2011; Pietrzak *et al.*, 2013), addiction (Bernard *et al.*, 2011), depression (Berridge and Waterhouse, 2003), suicidal behaviour (Roy *et al.*, 2017) and chronic pain (Llorca-Torralba *et al.*, 2016; Taylor and Westlund, 2017).

reminiscent of locally specific connectivity in dopaminergic nuclei (Haber and Knutson, 2010), tracing studies in the rat suggest that there might be distinct projections from rostralateral LC to hippocampus, amygdala and septum (Van Bockstaele *et al.*, 2006) and from caudal aspects of the LC to the spinal cord (Ennis *et al.*, 1991). This may indicate a stronger involvement of rostralateral LC in modulating memory encoding and caudal LC in modulating pain perception.

While the LC is among the first brain structures to demonstrate pathology in neurodegenerative diseases, it currently remains unclear how alterations in LC structure and function influence pathogenesis and symptom progression. In human studies, neuropsychiatric symptoms associated with LC activity, such as sleep dysfunction, agitation, anxiety, appetite dysfunction and depression, appear as elements of the early clinical phenotypes of neurodegenerative diseases (Assal and Cummings, 2002; Lanctôt *et al.*, 2017; Ehrenberg *et al.*, 2018). In animal models, lesions of the LC have been shown to exacerbate tau and amyloid- $\beta$  plaque deposition, leading to depletion of noradrenaline in LC target regions and impaired cognitive function (Heneka, 2006; Kalinin *et al.*, 2006, 2012; Jardanhazi-Kurutz *et al.*, 2010; Chalermpananupap *et al.*, 2017; Rorabaugh *et al.*, 2017). Whether the influence of LC degeneration on pathology is directly related to a dysregulation of noradrenaline, or indirectly related via neuroinflammatory mechanisms or alterations in additional LC neuromodulators, such as brain-derived neurotrophic factor or galanin, requires further investigation (Chalermpananupap *et al.*, 2017; Betts *et al.*, 2018). Interestingly, there is also evidence of noradrenergic hyperactivity in early disease (as reviewed by Weinshenker *et al.*, 2018), consistent with a number of reports of elevated levels of CSF noradrenaline and/or noradrenaline turnover in Alzheimer's disease (Palmer *et al.*, 1987; Hoogendijk *et al.*, 1999). Thus, hyperactivity in a structurally impaired LC might further accelerate the propagation of neuropathology in neurodegenerative disease via noradrenergic projections (Weinshenker, 2018). As such, early detection of LC decline using *in vivo* imaging techniques might contribute to earlier diagnosis, and support personalized pharmacological interventions to alleviate compensatory hyperactivity of the noradrenaline system and potentially slow down disease progression.

Recent advances in non-invasive neuroimaging techniques now permit the *in vivo* assessment of the LC using MRI (Sasaki *et al.*, 2006; Keren *et al.*, 2009; Clewett *et al.*, 2016; Betts *et al.*, 2017; Priovoulos *et al.*, 2018) opening the possibility to track LC changes as a biomarker for noradrenergic dysfunction. The utility of this approach for clinical research will depend on whether LC imaging in combination with established biomarkers, can help to better stage neurodegenerative diseases and characterize biomarker-positive individuals before the onset of dementia. LC imaging could also have important implications in clinical trials as a stratification tool for predicting treatment success of pharmacological intervention studies targeting the noradrenergic system. This article reports on the consensus reached at the first European Locus Coeruleus Imaging meeting held in

Magdeburg in 2018. It describes the challenges for establishing LC MRI measures as a biomarker for diagnosis and targeting therapeutic interventions in neurodegeneration and outlines a strategy for obtaining reliable, biologically validated and clinically suitable imaging approaches.

As discovered over a decade ago (Sasaki *et al.*, 2006), the LC is visualized using MRI scanning protocols that are sensitive to a paramagnetic compound called neuromelanin, which accumulates in noradrenergic neurons, and may be taken as an indicator of LC integrity (i.e. cell density). While neuromelanin-sensitive MRI is a relatively new technique, a number of studies have shown that MRI can detect signal differences in the LC between healthy controls and diseases with known LC involvement (e.g. in major depression, Parkinson's disease and Alzheimer's disease as recently reviewed by Liu *et al.*, 2017). Given, however, the substantial interindividual differences in LC measures across healthy older adults (Liu *et al.*, 2017, 2019), further studies are required to establish whether LC degeneration can be reliably detected *in vivo* (Liu *et al.*, 2017; Sulzer *et al.*, 2018). Furthermore, to clarify whether interindividual variability in LC integrity is related to varying levels of neuropathologies (e.g. tau, amyloid or  $\alpha$ -synuclein), studies using LC MRI in combination with *in vivo* measurements of pathology (e.g. PET and CSF biomarkers) in cognitively normal older adults and patients are required. While these studies are currently underway, first results in ageing and early-stage Alzheimer's disease indicate that LC MRI contrast is indeed modulated by both tau and amyloid pathology. Recent evidence demonstrating that LC MRI contrast is associated with CSF amyloid (amyloid- $\beta_{42/40}$ ) in early-stage Alzheimer's disease (Betts *et al.*, 2019) and tau pathology at higher levels of amyloid burden using tau and amyloid PET, respectively (Jacobs *et al.*, 2018a), may partially explain the interindividual variability in LC integrity observed in old age. Interestingly, post-mortem studies using  $^{18}\text{F}$ -AV-1451 tau PET have also shown off-target binding properties to neuromelanin in the substantia nigra (Marquié *et al.*, 2015; Hansen *et al.*, 2016). Thus  $^{18}\text{F}$ -AV-1451 may also be capable of imaging neurodegeneration. However, such changes may be difficult to interpret because of the mixed PET signal generated by on-target binding to tau tangles and off-target binding to neuromelanin, which would likely also be age-dependent.

## Practical considerations in *in vivo* LC imaging

The intrinsic neuromelanin-driven contrast that allows us to visualize the LC using MRI was first identified *in vivo* as hyperintensity on 2D T<sub>1</sub>-weighted turbo spin echo (TSE) images (Sasaki *et al.*, 2006). These hyperintensities correspond closely with areas of higher concentration of neuromelanin (Keren *et al.*, 2015), suggesting that the high signal intensities in the LC are driven by neuromelanin. In support

of this, a recent study has shown that the neuromelanin concentration in the substantia nigra is linearly related to neuromelanin-MRI contrast and resting blood flow in the substantia nigra (Cassidy *et al.*, 2019). The observation that LC MRI acquisitions are subject to incidental magnetization transfer (MT) effects (Dixon *et al.*, 1990) and that dedicated MT preparation increases neuromelanin-related contrast, have led several authors to credit MT as the primary source of LC contrast in MRI (Nakane *et al.*, 2008; Priovoulos *et al.*, 2018). Recent findings suggest that an interaction of (higher) intracellular water content with paramagnetic ions (such as neuromelanin) may set the LC apart from its surroundings in MT-weighted imaging (Watanabe *et al.*, 2019). Moreover, paramagnetic ions in addition to neuromelanin may contribute to this effect as structures low in neuromelanin (e.g. periaqueductal grey matter) demonstrate similar MRI contrast to the LC using MT-weighted imaging (Cassidy *et al.*, 2019; Watanabe *et al.*, 2019). Despite the different approaches that have successfully visualized the LC (Fig. 1), a precise understanding of the underlying contrast mechanism is thus still lacking. As outlined in more detail below, a combination of histological and post-mortem imaging studies would provide important insights in this regard. Mechanisms involving both neuromelanin concentration and macromolecules in the LC and surrounding tissues may be active simultaneously, and a combination of mechanisms may be required to explain the contrast patterns seen in normal ageing and in pathology. A relevant aspect for imaging neuromelanin is that it is known to scavenge metals both across the lifespan and in disease states (Zecca *et al.*, 2004; Biesemeier *et al.*, 2016). *In vitro* studies, albeit with synthetic melanin, suggest that  $T_1$  shortening in the LC may be driven by compounds of neuromelanin and chelated metals, such as iron and copper (Enochs *et al.*, 1989, 1997; Trujillo *et al.*, 2017) impacting the macromolecule-bound pool, rather than neuromelanin or iron alone (Langley *et al.*, 2015; Trujillo *et al.*, 2017). It has therefore been proposed that complexes of neuromelanin-bound paramagnetic ions are the primary drivers of LC contrast (Enochs *et al.*, 1989; Nakane *et al.*, 2008; Trujillo *et al.*, 2017); however, neuromelanin itself, even free of metals, is paramagnetic (Shima *et al.*, 1997). Indeed, at least *in vivo*, LC contrast does not seem to benefit from typical iron-sensitive contrasts, such as quantitative susceptibility mapping (QSM) or apparent  $R_2^*$  (Acosta-Cabronero *et al.*, 2016; Betts *et al.*, 2016, respectively) (Fig. 1N and R).

More recently, MT preparation and/or  $T_1$ -weighting have been combined, both with short repetition time spoiled gradient echo and turbo-flash readouts, to increase spatial resolution and/or shorten the acquisition time compared to TSE acquisitions (Chen *et al.*, 2014; Betts *et al.*, 2017; Hämmerer *et al.*, 2018; Priovoulos *et al.*, 2018). The small size of the LC has motivated the use of high spatial resolution, at least in-plane, while high isotropic resolution minimizes partial volume effects (i.e. inclusion of non-LC tissue within a putative LC voxel). However, this comes at

the cost of relatively low signal- and contrast-to-noise ratio (SNR and CNR, respectively) due to smaller voxel sizes and higher vulnerability to subject motion, which has prompted averaging over multiple repetitions. Anisotropic voxels, which mimic the shape and orientation of the LC, have capitalized on the elongated shape of the LC to increase SNR and shorten scan times. Given the tilted and not perfectly cylindrical nature of the LC, this strategy is prone to errors at the most rostral and caudal ends of the structure leading to biases in segmentation and volumetric measurements (Liu *et al.*, 2017). Alternatively, isotropic acquisitions that capture the entire rostrocaudal length of the LC have also been proposed (Betts *et al.*, 2017; Priovoulos *et al.*, 2018) and may be more consistent with *ex vivo* measurements compared to anisotropic scans (Liu *et al.*, 2017). While the increased SNR with ultra-high field MRI (i.e.  $\geq 7.0$  T) offers higher attainable spatial resolution and/or shorter acquisition times, increased specific absorption rates means that higher power acquisitions, e.g. those using MT preparation pulses or high flip angles, might not be readily available thereby necessitating further optimization (Priovoulos *et al.*, 2018) (see also Box 2 for recommendations on how to use currently available sequences).

## Validating *in vivo* locus coeruleus imaging using post-mortem MRI and histology

A key aim of conducting LC imaging in clinical groups is to capture *in vivo* disease-related physiological and structural changes such as reductions in neuronal density. Several validation strategies, including a combination of post-mortem magnetic resonance microscopy and histological labelling (Forstmann *et al.*, 2017), have thus been proposed to shed new light into the underlying biological processes driving *in vivo* imaging results. Such approaches, however, are also technically challenging. Tissue fixation and embedding media can affect the properties of post-mortem tissue and strongly influence the MRI signal (Dusek *et al.*, 2019). Thus, the same tissue properties might be expressed differently in post-mortem and *in vivo* MRI. For instance, tissue fixation causes strong  $T_1$  and  $T_2$  shortening that is additionally dependent on the choice of fixative agent and fixation time (Birkel *et al.*, 2016, 2018). Contrast changes also arise if the temperature used for post-mortem scanning differs from 37°C (Birkel *et al.*, 2014). Differences between *in vivo* and post-mortem tissue could also be driven by changes in metal oxidation states during fixation or by redistribution of iron and other metals across macromolecules (e.g. proteins, neuromelanin, etc.) (Shima *et al.*, 1997; Krebs *et al.*, 2014). It should be considered that iron is bound in brain tissue in different molecular forms such as ferritin, neuromelanin, hemosiderin and others,

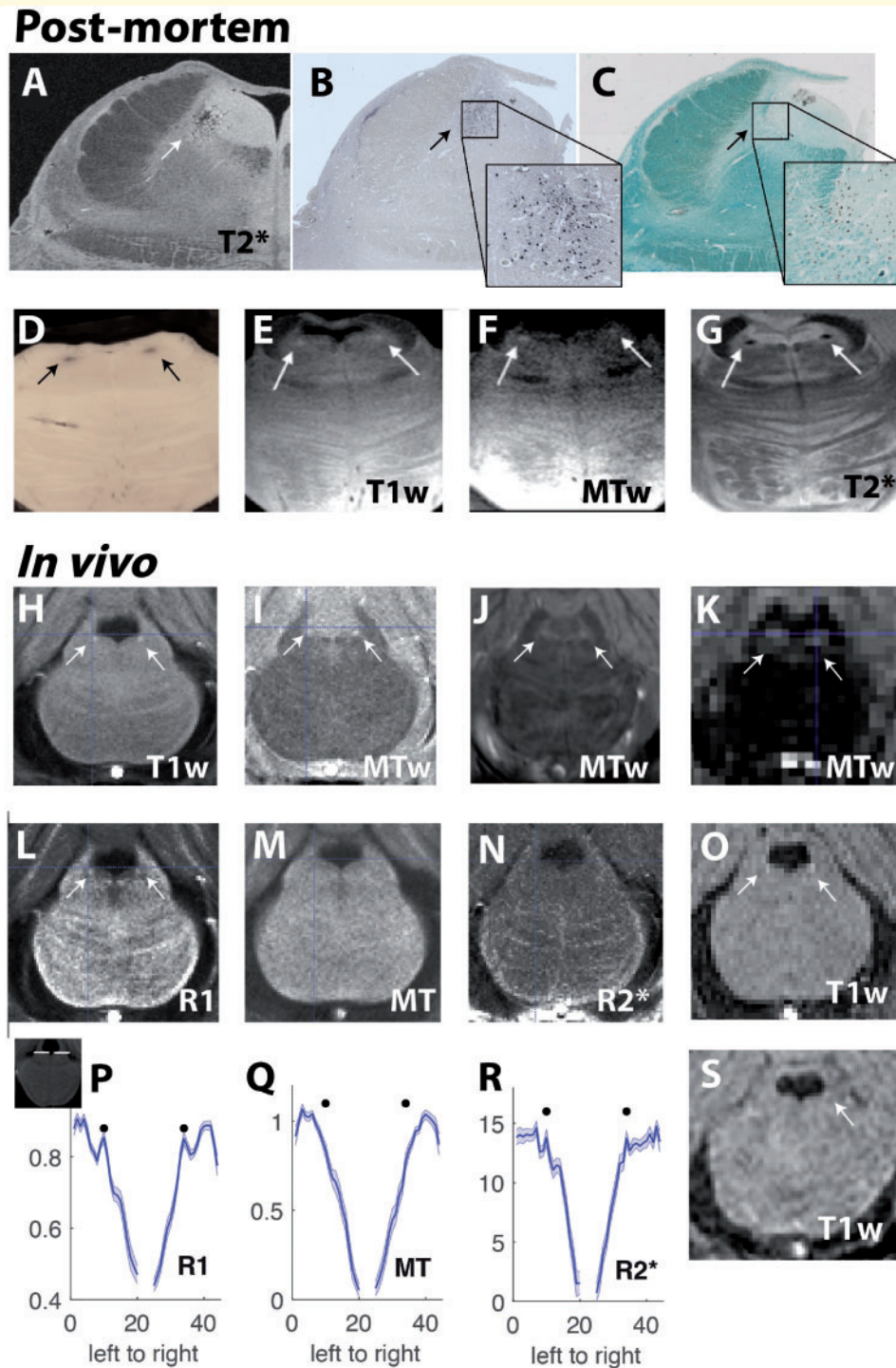


**Figure 1 Overview of LC visibility using post-mortem and *in vivo* MRI.** The LC can be imaged in post-mortem tissue using numerous MRI protocols [arrows indicate the LC, evident as dark spots in  $T_2^*$  (**A** and **G**) and bright spots in  $T_1$ -weighted (**E**) and MT-weighted (**F**) scans] in addition to using histological techniques. (**D**) The LC is visible as dark spots in a post-mortem slice without any staining, due to neuromelanin deposits, which are thought to contribute to magnetic resonance visibility of the LC. (**C**) Myelination in the LC area. The LC and central pontine grey show very low myelination, but are surrounded by areas with very high and intermediate myelination (green areas), possibly also contributing to MR visibility of the LC. To image the LC *in vivo*,  $T_1$ -weighted (**H**, **O** and **S**) and MT-weighted (**I–K**) MRI protocols can be used (arrows indicate the LC, evident as bright spots in  $T_1$ -weighted and MT-weighted scans). Using these protocols, a decline in LC integrity in Alzheimer's disease dementia (**S**) compared to healthy elderly adults (**O**) can be identified (Betts et al., 2019). To fine-tune these scan protocols further, it is necessary to understand the magnetic resonance contrast mechanisms that underlie LC visibility. (**L–N** and **P–R**) Quantitative maps which isolate different magnetic resonance contrast effects ( $R_1$ , MT and  $R_2^*$  effects), show that LC visibility in  $T_1$ -weighted as well as MT-weighted scans *in vivo* is mostly due to  $R_1$  effects (mean LC visibility across 22 healthy older adults extracted from line regions of interest; see inset on *right* for position of line regions of interest. Black dots indicate position of maximal signal intensity based on  $T_1$ -weighted maps. Peaks in signal intensity are apparent in  $R_1$

(continued)

each having different physico-chemical properties (Ward *et al.*, 2014). Thus, LC contrast observed *in vivo* using neuromelanin-sensitive MRI at clinical field strength cannot be easily replicated with post-mortem magnetic resonance microscopy at lower temperature ( $T \leq 21^\circ\text{C}$ ) and ultra-high magnetic field strengths ( $\geq 7.0\text{ T}$ ). In particular,  $T_2^*/R_2^*$  measurements of the LC return markedly different values *in vivo* and post-mortem tissue. While they often afford the best visibility in post-mortem tissue (Fig. 1A and G),  $T_2^*$  effects are not evident in individual *in vivo* samples and are comparatively weaker than  $R_1$  effects in group analyses (Fig. 1L–N and P–R). However, by adjusting acquisition parameters, it is still possible to observe the characteristic  $T_1$ - and MT-weighted hyperintensity of the LC in *in vivo* (Fig. 1H–K, O and S) and *ex vivo* MRI (Fig. 1E and F). To address comparability issues, future post-mortem MRI studies focusing on the LC could combine quantitative  $T_1$ ,  $T_2^*$ , MT and QSM with tight control of the post-mortem fixation time and iron and metal concentrations in the fixation solution in order to relate magnetic resonance signal intensities to stereological and quantitative histological measures (e.g. myelin, lipids, neurons, iron, neuromelanin, copper, and iron- and copper-containing proteins).

Using a combination of histology and post-mortem MRI in the LC, a recent study explored whether neuromelanin-sensitive MRI contrast could serve as a proxy measure of LC ‘integrity’ (i.e. neuronal density in the LC). The authors showed that areas of LC hyperintensity in  $T_1$ -weighted MRI were co-localized with neuromelanin-rich neurons in the LC region (Keren *et al.*, 2015), suggesting that LC visibility in MRI may indeed be driven by the neuromelanin content of noradrenergic neurons. Similarly, studies using neuromelanin-sensitive MRI could show that age-related cross-sectional patterns in *in vivo* signal intensity across the lifespan (Shibata *et al.*, 2006; Jacobs *et al.*, 2018a; Liu *et al.*, 2019) replicate the inverted U-shaped cross-sectional development of neuromelanin deposits in the LC observed in post-mortem tissue (Mann and Yates 1974, but see Ohm *et al.*, 1997; Zecca *et al.*, 2004 for studies reporting a stable level of neuromelanin-containing neurons or linear increase of neuromelanin content in LC tissue across the lifespan, respectively). This inverted U-shaped pattern has been suggested to reflect increasing neuromelanin content due to continuous noradrenaline production during adulthood prior to ensuing cell death and clearance

of released intracellular neuromelanin with the advent of age-related neurodegeneration and onset of disease (Mann and Yates, 1974). Indeed, post-mortem data suggest that neuromelanin may be a more suitable indicator of neuronal density in older adults (at least  $> 55$  years) as younger adults’ LC neurons may not yet be sufficiently pigmented with neuromelanin to allow inference on cell numbers in neuromelanin-sensitive MRI (Manaye *et al.*, 1995; Liu *et al.*, 2019). Nonetheless, further studies are warranted to investigate whether higher signal intensities in older adults invariably represent more intact LC neurons in the LC, and whether additional mediating factors for interpreting LC-related MRI signals must be considered in different age groups or clinical populations. For instance, pathologically altered proteins, such as hyperphosphorylated or aggregated tau, which are well known markers of ageing and neurodegenerative disease as well as non-pathological proteins and lipids, are additional important constituents of neuromelanin pigments (Engelen *et al.*, 2012; Zucca *et al.*, 2018) that accumulate in specific organelles in the LC as occurs in substantia nigra (Zecca *et al.*, 2004; Braak *et al.*, 2011; Zucca *et al.*, 2017). However, the effect of these constituents on LC MRI contrast has not yet been systematically explored.

## Outlook and conclusion

A major goal of *in vivo* LC imaging in clinical research is to aid differential diagnosis, disease monitoring and stratification to novel treatments. As such, LC imaging has the potential to become a component of a precision medicine approach to neurodegenerative diseases. As brain function adapts to ensuing pathology, such as receptor increases in target areas of noradrenergic LC projections or increased connectivity following a decline in LC function (Herrmann *et al.*, 2004; Ye *et al.*, 2015), LC imaging could provide a stratification tool for predicting treatment success of pharmacological intervention studies targeting the noradrenergic system (Ye *et al.*, 2015, see also Fig. 2). Once its relationship to pathogenic changes (e.g.  $\alpha$ -synuclein or tau aggregation) has been determined, it could also support differential diagnosis and be added to the portfolio of longitudinal monitoring staging tools for neurodegenerative diseases. Over the next years, we expect substantial progress towards these goals through a multidisciplinary

### Figure 1 Continued

and to some extent in  $R_2^*$  maps (Hämmerer *et al.*; 2018a)]. Sequence details/ stains: (A) 7 T  $T_2^*$ -weighted (50  $\mu\text{m}$  resolution) FLASH MRI image (TE = 19 ms); (B) TH staining for LC neurons (dark); (C) Luxol fast blue staining for myelinated fibres in same slice (green); (D) Block face image after celloidin embedding (LC neurons dark); (E) 7 T  $T_1$ -weighted (0.2  $\times$  0.2  $\times$  2 mm) TSE image (TE/TR/TI = 11/3000/825 ms); (F) 7 T MT-weighted FLASH MRI image (TE/TR = 5.1/26 ms); (G) 7 T  $T_2^*$ -weighted FLASH image (TE/TR = 21/30 ms) (Otaduy *et al.*, unpublished results); (H) 3 T  $T_1$ -weighted (0.4  $\times$  0.4  $\times$  3 mm) FLASH image (TE/TR = 3.35–16.95/27) averaged across six repetitions; (I) 3 T MT-weighted (0.4  $\times$  0.4  $\times$  3 mm) FLASH image (TE/TR = 3.35–16.95/30.74); (J) 7 T MT-TFL image (0.4  $\times$  0.4  $\times$  0.5 mm); (K) 3 T MT-weighted (1.5 mm<sup>3</sup>) SPGR image (TE/TR = 5 ms/30 ms); (O and S) 3 T  $T_1$ -weighted (0.75 mm<sup>3</sup>) FLASH image (TE/TR = 5.56 ms/20 ms). Image in J is reproduced with permission from Priovoulos *et al.* (2018); O is reproduced with permission from Betts *et al.* (2017). TE/TR/TI = echo time/repetition time/inversion time.

## Box 2 Practical suggestions for *in vivo* LC imaging

### Sequences

The LC is most visible using T<sub>1</sub>- or MT-weighted structural sequences and can be well characterized using 3 T and 7 T MRI (see Betts *et al.*, 2017; Priovoulos *et al.*, 2018 and Liu *et al.*, 2017 for a recent review). To date, there is no single 'best' sequence for LC imaging: there is a trade-off between non-quantitative protocols offering easier LC localization, and quantitative magnetic resonance acquisitions that provide more objective biophysical measures of brain tissue but with lower localization ability compared to dedicated LC sequences.

### Voxel size

Owing to the small size of the LC (~15 mm in length and 1–3 mm in diameter), larger voxel sizes should be avoided as they result in weaker signals owing to partial volume effects with tissue outside the LC within the voxel. On the other hand, voxel volumes lower than 0.4–0.5 mm<sup>3</sup> run the risk of lacking sufficient signal-to-noise ratio, given the current sensitivity of neuromelanin-sensitive magnetic resonance sequences. If more accurate LC volume assessments (with less partial volume contamination) are desired, isotropic voxel sizes are preferable [e.g. 0.75 mm × 0.75 mm × 0.75 mm are possible at 3 T (Betts *et al.*, 2017) and 0.4 mm × 0.4 mm × 0.5 mm at 7 T (Priovoulos *et al.*, 2018)]. These, however, can make identification of individual LCs harder because of lower signal-to-noise ratio, requiring a group template approach (see below). If reliable identification of individual LCs is desired but accurate volume assessments are less critical, anisotropic voxel sizes (e.g. 0.5 mm × 0.5 mm in plane resolution × 2 mm slice thickness) can be used to exploit the quasi-cylindrical shape of the LC and maximize signal-to-noise ratio at the cost of greater partial volume errors in peripheral LC voxels (Liu *et al.*, 2017).

### Acquisition

It is recommended that the field-of-view is aligned perpendicular to the dorsal edge of the pons such that cylindrical voxels align with the LC.

### Motion artefacts

Great care should be taken to reduce head motion during the MRI acquisition. A thin pillow placed on the base of the coil to ensure tight fixation and patient comfort can help minimize motion and achieve high measurement precision e.g. improving coregistration across/within individuals e.g. between structural and functional data. Shorter acquisition times which are less prone to motion artefacts can be achieved by using a reduced field-of-view comprising the brainstem only and by relying on offline-averaging of scans (Chen *et al.*, 2014). Typical scan durations for smaller field-of-view acquisitions take approximately half the time of whole-brain acquisitions and range between 5 and 9 min at 3 T and 7 T MRI, respectively (Liu *et al.*, 2017; Priovoulos *et al.*, 2018). However, template-based segmentation approaches (see below) are more challenging with reduced field-of-view acquisitions than with whole brain scans (but see Dahl *et al.*, 2019).

### Post-processing

Semi-automated LC segmentation can be performed through highly iterative co-registration resulting in a high definition group-average template where the LC can be reliably identified. The resultant template LC region of interest can then be spatially transformed to each individual's native space (Betts *et al.*, 2017; Liu *et al.*, 2019). When using template-based approaches however, care must be taken to minimize the impact of coregistration inaccuracies and additional user intervention might be required. There are at present differing views on whether LC segmentation should be performed manually or automatically, and on whether LC measurements should encompass the whole structure or favour partial extraction to avoid potential contamination. Chen *et al.* (2014) argued that automated segmentation approaches might be less error-prone and may thus lead to higher consistency across scans and studies, and that visually locating the LC as the highest-intensity voxel at either side of the fourth ventricle (on the axial plane) might be susceptible to noise-related errors. In contrast, Keren *et al.* (2009) argued that assessing single voxels might be more reliable in that it does not rely on boundary definitions or signal intensity thresholding, thereby leading to improved sensitivity to overall LC differences. To date, however, no study has systematically compared manual and automated methods.

### Reference normalization

An important limitation of MRI is that it produces arbitrarily scaled greyscale images that are suboptimal for intersubject comparisons because normalization to a proximal control region (often the pontine tegmentum) becomes necessary (Betts *et al.*, 2017; Liu *et al.*, 2017; Hämmerer *et al.*, 2018). However, the reference tissue may also change throughout the lifespan, or be abnormal in neurodegenerative diseases (Keren *et al.*, 2009; Clewett *et al.*, 2016). Furthermore, asymmetric signal-intensity biases in the LC and surrounding tissue have been reported both in healthy subjects and Parkinson's disease patients (Keren *et al.*, 2009; Garcia-Lorenzo *et al.*, 2013; Betts *et al.*, 2017; Tona *et al.*, 2017), in apparent contradiction with post-mortem studies that show largely symmetric distributions of neuromelanin-pigmented cells in the LC (German *et al.*, 1988; Baker *et al.*, 1989; Chan-Palay and Asan, 1989; Ohm *et al.*, 1997). It is therefore imperative to avoid instrumental biases such as transmit and receive field inhomogeneities, and ensure asymmetries are not introduced by the methodology. To this end, quantitative (parametric) MRI (Weiskopf *et al.*, 2013) has shown promise by quantifying specific tissue properties in terms of physical units and may now be used for quantitative LC imaging (Fig. 1L–N and P–R) (Hämmerer *et al.*, 2018a). Moving forward, one may speculate that multi-parametric mapping might be preferred to single-contrast assessments for a more complete view of LC status and greater insight into underlying contrast mechanisms, especially if performed within the population-specific time constraints.

### Age comparisons and control groups

Owing to an age-related increase in neuromelanin content in LC cells as well as LC signal intensity using neuromelanin-sensitive MRI, LC imaging may be suboptimal in younger adults, likely due to reduced neuromelanin levels compared to older adults (Zecca *et al.*, 2004, 2006; Liu *et al.*, 2019). For the same reason, interpreting age differences in LC MRI contrast between young and older adults as age differences in LC integrity may be problematic. In a large cross-sectional dataset, a decline in LC integrity was only observed at ~60 years of age and over (Liu *et al.*, 2019). At present it is unclear if neuromelanin-sensitive MRI can detect a reduction in LC integrity below this age range. Moreover, within an ageing sample, control groups must be tightly matched for age to the clinical population under investigation.



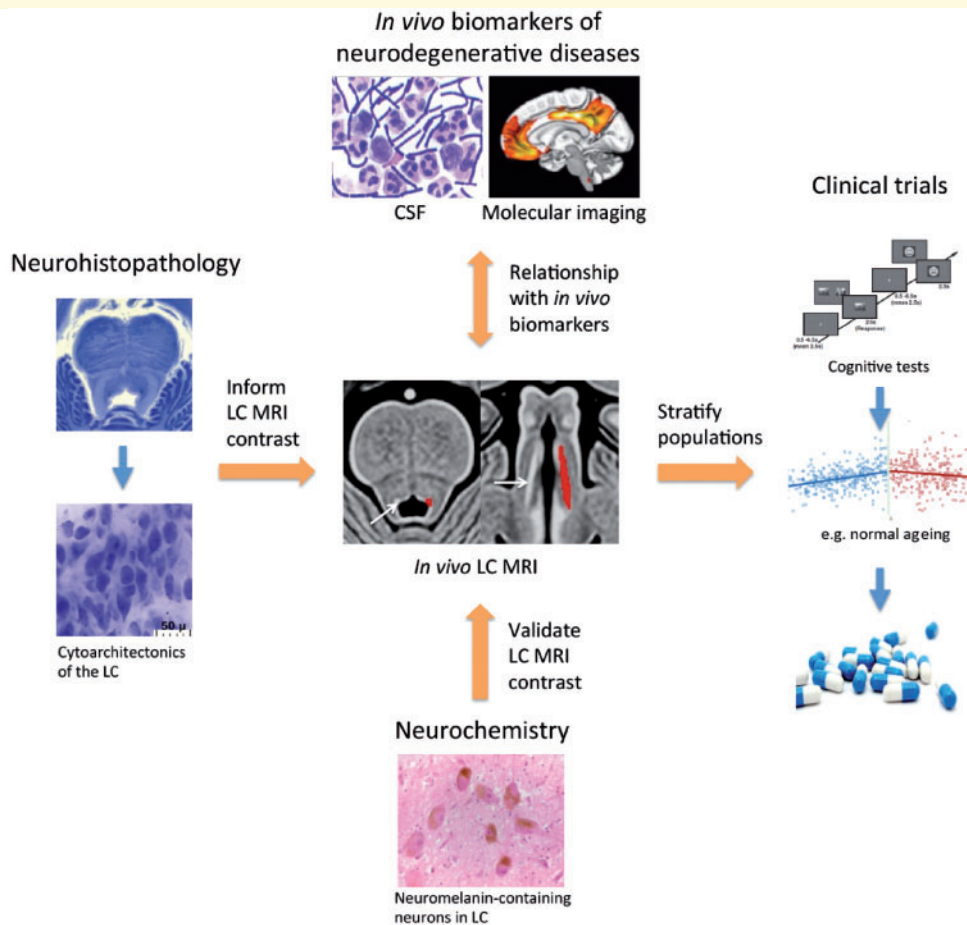


**Figure 2 Establishing LC imaging as a biomarker for noradrenergic dysfunction.** LC imaging offers potential as a disease monitoring and stratification tool to predict the success of novel pharmacological ligands in clinical trials. To achieve this aim, it will be essential to validate *in vivo* LC MRI contrast with respect to the concentration of neuromelanin and density of noradrenergic neurons in post-mortem tissue. This will be important for developing a deeper understanding into how changes in LC MRI contrast both *in vivo* and in post-mortem tissue correlate with neuromelanin-bound metals in noradrenergic neurons and is influenced by the neuropathological characteristics of neurodegenerative diseases. In the clinic, longitudinal LC imaging may be combined with biomarkers (e.g. in CSF or molecular imaging) to assess how changes in LC MRI contrast may drive clinical and pathological manifestations of neurodegenerative diseases. Source of CSF image: Wikimedia Commons; molecular imaging figure is adapted from Palmqvist *et al.* (2017); LC integrity image (*middle*) adapted with permission from Betts *et al.* (2017); age effects on LC integrity image (*right*) reproduced with permission from Liu *et al.* (2019).

collaboration of experts in neurodegenerative diseases, imaging, neuropathology and cognition.

As neuromelanin accumulates in the cell bodies of LC neurons, neuromelanin-sensitive MRI can only inform on changes in cell density but not changes in synaptic density or cell activity. It is known from post-mortem studies that cell numbers in the LC decline with advancing Alzheimer's disease pathology (Theofilas *et al.*, 2017). However, prior to cell loss, changes in synaptic density in the LC and/or neuronal activity should be considered. Post-mortem and lesion studies suggest that noradrenaline production in remaining LC neurons may increase following degeneration of LC neurons (for a review see Weinshenker *et al.*, 2018). At present, it is not known whether synaptic density is altered prior to or in tandem with cell loss in the LC. It would be interesting to use novel PET tracers of synaptic density (Finnema *et al.*, 2016) in combination with LC

imaging to assess how differences in LC synapse density relate to LC MRI contrast in neurodegenerative diseases. Direct and indirect functional measures of LC activity or noradrenaline release can be assessed using high resolution functional MRI, pupillometry, PET measures of noradrenergic transporter levels (Sommerauer *et al.*, 2018), or by assessing noradrenaline levels in CSF. These measures, however, are not short of caveats. PET and functional MRI measures provide noisy assessments given the small size of the LC. Moreover, the LC is also known to release dopamine and GABA (Kempadoo *et al.*, 2016; Takeuchi *et al.*, 2016; Breton-Provencher and Sur, 2019), thus dopamine and GABA levels may also need to be assessed in conjunction with noradrenaline levels when characterizing LC function. Finally, it can also be difficult interpreting functional activation in the LC as an indicator of neuronal capacity since activation will not only depend on the

number of neurons or synaptic density, but also on the degree in which the LC is engaged during the processing of the task at hand [i.e. the strength and the nature of the experimental manipulation, e.g. as suggested previously by Hämmerer *et al.* (2018)]. Nonetheless, synaptic density and functional activation may be superior indicators of cognitive impairment than cell pathology (Terry *et al.*, 1991). As the specificity of functional and experimental manipulations for the LC increases, these measures may contribute valuable additional data on the role of the LC in neurodegenerative diseases.

One of the main tasks ahead for LC research lies in setting up carefully designed longitudinal studies in healthy ageing and disease cohorts with deep cognitive and physiological phenotyping (e.g. the DELCODE study; Jessen *et al.*, 2018) to assess how LC integrity is related to cognitive symptoms and functional brain changes at the earliest stages of neurodegeneration. Previous work assessing the reproducibility of LC imaging by quantifying the stability of LC contrast across two or more independent scan sessions has revealed moderate to high reproducibility (Langley *et al.*, 2017; Tona *et al.*, 2017; Betts *et al.*, 2017; Dahl *et al.*, 2019). Therefore to achieve reliable longitudinal testing in the future will require an improvement in the reproducibility and reliability of LC imaging techniques. To assess how the LC modulates the function of distributed brain networks at rest and during cognitive tasks, will require further optimization of existing functional MRI sequences to overcome the challenges of brainstem imaging (Düzel *et al.*, 2015) and inclusion of additional physiological information (see Liu *et al.*, 2017 for recommendations). In addition, experimental tasks that elicit robust LC signals require development (Mather *et al.*, 2016; Liu *et al.*, 2017; Clewett *et al.*, 2018).

Second, future studies should test whether LC imaging is related to disease progression in neurodegenerative diseases. This will require characterizing the relationship between LC MRI measures and neuropathology (e.g. with respect to amyloid, tau or alpha-synuclein using CSF biomarkers or PET) but also noradrenergic function using noradrenergic PET-tracers including those to assess noradrenergic transporter density (Sommerauer *et al.*, 2018). However, advances in analysis (to maximize spatial resolution) and exclusion of potential off-target binding sites (Lee *et al.*, 2018) must accompany ligand development. For optimizing and validating LC MRI further, greater synergy between *in vivo*, post-mortem, *in vitro* and clinical studies is required for a deeper understanding into how LC MRI contrast relates to the pathophysiology of different neurodegenerative diseases (Fig. 2). Such studies will also benefit from using clinically informed test beds, i.e. populations, that show a clear difference in relevant tissue properties, e.g. between young and older adults but also in neurodegenerative diseases, such as Alzheimer's disease and beyond (Box 1).

Finally, a growing body of knowledge on similarities and differences between neuromelanin deposits in noradrenergic

cells in the LC and dopaminergic cells in the substantia nigra (Zecca *et al.*, 2004; Zucca *et al.*, 2006; Wakamatsu *et al.*, 2015) open further avenues for using *in vivo* neuromelanin-sensitive MRI to also investigate the involvement of the substantia nigra in tandem with the LC in a wide range of clinical conditions, i.e. in diseases also affecting the dopaminergic system, such as Parkinson's disease (Sulzer *et al.*, 2018).

In conclusion, there is rapid progress towards achieving more sensitive and high-resolution *in vivo* imaging of the LC. The methods are non-invasive and fast enough to be well tolerated using high (3T) or ultra-high ( $\geq 7$ T) MRI, and can have great potential to inform the effectiveness of psychopharmacological probes, therapeutic trials, and physiological monitoring in clinical populations. We anticipate rapid growth in the evidence base for developing LC imaging as a biomarker in neurodegenerative diseases.

## Funding

M.B. and D.H. were supported by the Human Brain Project (SP3 WP 3.3.1) and CRC 779 (Project A7). E.D. and D.H. are also supported by the MRC MR/P012698/1. L.Z. and F.A.Z. were supported by the Italian Ministry of Education, University, and Research (MIUR) - National Research Programme (PNR) - National Research Council of Italy (CNR) Flagship "InterOmics" Project (PB.P05), by MIUR - PNR - CNR Aging program 2012-2014. L.Z. was also supported by the Grigioni Foundation for Parkinson's Disease (Milan, Italy). C.L. is supported by the MRC (MR/R006504/1) and L.P. is supported by the MRC (MR/P01271X/1). J.R. is supported by the MRC, NIHR, Wellcome Trust (103838), McDonnell Foundation, AZ-Medimmune and Janssen. M.M. is supported by the German Research Foundation (DFG) priority program PP 2041 (MO 2249/3-1) and the Alzheimer-Forschungs-Initiative e.V., (AFI # 18072). H.J. is supported by a NWO VENI grant [451-14-035], a standard grant of Alzheimer Nederland [#15007] and by European Union's Horizon 2020 Research and Innovation Programme under the Marie Skłodowska-Curie Grant agreement [IF-2015-GF, 706714]. N.W. received funding from the European Research Council under the European Union's Seventh Framework Programme (FP7/2007-2013) / ERC grant agreement n° 616905, and from the European Union's Horizon 2020 research and innovation programme under the grant agreement No 681094, and from the BMBF (01EW1711A & B) in the framework of ERA-NET NEURON. H.R.S. holds a 5-year professorship in precision medicine at the Faculty of Health Sciences and Medicine, University of Copenhagen, which is sponsored by the Lundbeck Foundation (Grant Nr. R186-2015-2138). L.T.G. is funded by NIH R01AG056573, K24AG053435 and the BrightFocus Foundation. R.H. is supported by the UCLH NIHR Biomedical Research Centre. K.F. is supported by the German Research Foundation (DFG)

project FL715-1-3. The Wellcome Centre for Human Neuroimaging is supported by core funding from the Wellcome (203147/Z/16/Z).

## Competing interests

H.R.S. has received honoraria as speaker from Sanofi Genzyme, Denmark and Novartis, Denmark, as a consultant from Sanofi Genzyme, Denmark and as senior editor (NeuroImage) from Elsevier Publishers, Amsterdam, The Netherlands. H.R.S. has also received royalties as book editor from Springer Publishers, Stuttgart, Germany. The Max Planck Institute for Human Cognitive and Brain Sciences has an institutional research agreement with Siemens Healthcare.

## References

- Acosta-Cabronero J, Betts MJ, Cardenas-Blanco A, Yang S, Nestor PJ. In vivo MRI mapping of brain iron deposition across the adult lifespan. *J Neurosci* 2016; 36: 364–74.
- Andrés-Benito P, Fernández-Dueñas V, Carmona M, Escobar LA, Torrejón-Escribano B, Aso E, et al. Locus coeruleus at asymptomatic early and middle Braak stages of neurofibrillary tangle pathology. *Neuropathol Appl Neurobiol* 2017; 43: 373–92.
- Arendt T, Brückner MK, Morawski M, Jäger C, Gertz H-J. Early neurone loss in Alzheimer's disease: cortical or subcortical? *Acta Neuropathol Commun* 2015; 3: 10.
- Assal F, Cummings JL. Neuropsychiatric symptoms in the dementias. *Curr Opin Neurol* 2002; 15: 445–50.
- Aston-Jones G, Bloom FE. Activity of norepinephrine-containing locus coeruleus neurons in behaving rats anticipates fluctuations in the sleep-waking cycle. *J Neurosci* 1981; 1: 876–86.
- Aston-Jones G, Cohen JD. An integrative theory of locus coeruleus-norepinephrine function: adaptive gain and optimal performance. *Annu Rev Neurosci* 2005; 28: 403–50.
- Baker KG, Törk I, Hornung J-P, Halasz P. The human locus coeruleus complex: an immunohistochemical and three dimensional reconstruction study. *Exp Brain Res* 1989; 77: 257–70.
- Benarroch EE. The locus ceruleus norepinephrine system Functional organization and potential clinical significance. *Neurology* 2009; 73: 1699–704.
- Benarroch EE, Schmeichel AM, Low PA, Sandroni P, Parisi JE. Loss of A5 noradrenergic neurons in multiple system atrophy. *Acta Neuropathol (Berl)* 2008; 115: 629–34.
- Bernard R, Kerman IA, Thompson RC, Jones EG, Bunney WE, Barchas JD, et al. Altered expression of glutamate signaling, growth factor and glia genes in the locus coeruleus of patients with major depression. *Mol Psychiatry* 2011; 16: 634–46.
- Berridge CW, Waterhouse BD. The locus coeruleus–noradrenergic system: modulation of behavioral state and state-dependent cognitive processes. *Brain Res Rev* 2003; 42: 33–84.
- Betts MJ, Acosta-Cabronero J, Cardenas-Blanco A, Nestor PJ, Düzel E. High-resolution characterisation of the aging brain using simultaneous quantitative susceptibility mapping (QSM) and R2\* measurements at 7T. *NeuroImage* 2016; 138: 43–63.
- Betts MJ, Cardenas-Blanco A, Kanowski M, Jessen F, Düzel E. In vivo MRI assessment of the human locus coeruleus along its rostrocaudal extent in young and older adults. *NeuroImage* 2017; 163: 150–59.
- Betts MJ, Cardenas-Blanco A, Kanowski M, Spottke A, Teipel SJ, Kilimann I, et al. Locus coeruleus MRI contrast is reduced in Alzheimer's disease dementia and correlates with CSF A $\beta$  levels. *Alzheimers Dement Diagn Assess Dis Monit* 2019; 11: 281–5.
- Betts MJ, Ehrenberg AJ, Hämmerer D, Düzel E. Commentary: Locus Coeruleus Ablation Exacerbates Cognitive Deficits, Neuropathology, and Lethality in P301S Tau Transgenic Mice. *Front Neurosci* 2018; 12: 401.
- Biesemeier A, Eibl O, Eswara S, Audinot J-N, Wirtz T, Pezzoli G, et al. Elemental mapping of Neuromelanin organelles of human Substantia Nigra: correlative ultrastructural and chemical analysis by analytical transmission electron microscopy and nano-secondary ion mass spectrometry. *J Neurochem* 2016; 138: 339–53.
- Birkel C, Langkammer C, Golob-Schwarzl N, Leoni M, Haybaeck J, Goessler W, et al. Effects of formalin fixation and temperature on MR relaxation times in the human brain: Formalin fixation MR relaxation mechanisms. *NMR Biomed* 2016; 29: 458–65.
- Birkel C, Langkammer C, Haybaeck J, Ernst C, Stollberger R, Fazekas F, et al. Temperature-induced changes of magnetic resonance relaxation times in the human brain: a postmortem study: temperature dependency of relaxation times in postmortem brain. *Magn Reson Med* 2014; 71: 1575–80.
- Birkel C, Soellradl M, Toeglhofer AM, Krassnig S, Leoni M, Pirpamer L, et al. Effects of concentration and vendor specific composition of formalin on postmortem MRI of the human brain: formalin and postmortem brain MRI. *Magn Reson Med* 2018; 79: 1111–5.
- Braak H, Del Tredici K. Where, when, and in what form does sporadic Alzheimer's disease begin? *Curr Opin Neurol* 2012; 25: 708–14.
- Braak H, Del Tredici K, Rüb U, de Vos RA, Steur ENJ, Braak E. Staging of brain pathology related to sporadic Parkinson's disease. *Neurobiol Aging* 2003; 24: 197–211.
- Braak H, Ghebremedhin E, Rüb U, Bratzke H, Del Tredici K. Stages in the development of Parkinson's disease-related pathology. *Cell Tissue Res* 2004; 318: 121–34.
- Braak H, Thal DR, Ghebremedhin E, Del Tredici K. Stages of the pathologic process in Alzheimer disease: age categories from 1 to 100 years. *J Neuropathol Exp Neurol* 2011; 70: 960–9.
- Breton-Provencher V, Sur M. Active control of arousal by a locus coeruleus GABAergic circuit. *Nat Neurosci* 2019; 22: 218–28.
- Brunnström H, Friberg N, Lindberg E, Englund E. Differential degeneration of the locus coeruleus in dementia subtypes. *Clin Neuropathol* 2011; 30: 104–10.
- Cassidy CM, Zucca FA, Girgis RR, Baker SC, Weinstein JJ, Sharp ME, et al. Neuromelanin-sensitive MRI as a noninvasive proxy measure of dopamine function in the human brain. *Proc Natl Acad Sci* 2019; 116: 5108–17.
- Chalermpananupap T, Schroeder JP, Rorabaugh JM, Liles LC, Lah JJ, Levey AI, et al. Locus coeruleus ablation exacerbates cognitive deficits, neuropathology, and lethality in P301S tau transgenic mice. *J Neurosci* 2017: 1483–17.
- Chan-Palay V, Asan E. Alterations in catecholamine neurons of the locus coeruleus in senile dementia of the Alzheimer type and in Parkinson's disease with and without dementia and depression. *J Comp Neurol* 1989; 287: 373–92.
- Chen X, Huddleston DE, Langley J, Ahn S, Barnum CJ, Factor SA, et al. Simultaneous imaging of locus coeruleus and substantia nigra with a quantitative neuromelanin MRI approach. *Magn Reson Imaging* 2014; 32: 1301–6.
- Clewett DV, Huang R, Velasco R, Lee T-H, Mather M. Locus coeruleus activity strengthens prioritized memories under arousal. *J Neurosci* 2018; 38: 1558–74.
- Clewett DV, Lee T-H, Greening S, Ponzio A, Margalit E, Mather M. Neuromelanin marks the spot: identifying a locus coeruleus biomarker of cognitive reserve in healthy aging. *Neurobiol Aging* 2016; 37: 117–26.
- Dahl MJ, Mather M, Düzel S, Bodammer NC, Lindenberger U, Kühn S, et al. Locus coeruleus integrity preserves memory performance across the adult life span. *bioRxiv* 2019. <https://www.biorxiv.org/content/10.1101/332098v3>.
- Dickson DW, Fujishiro H, DelleDonne A, Menke J, Ahmed Z, Klos KJ, et al. Evidence that incidental Lewy body disease is pre-

- symptomatic Parkinson's disease. *Acta Neuropathol (Berl)* 2008; 115: 437–44.
- Dixon WT, Engels H, Castillo M, Sardashti M. Incidental magnetization transfer contrast in standard multislice imaging. *Magn Reson Imaging* 1990; 8: 417–22.
- Dusek P, Madai VI, Huelnhagen T, Bahn E, Matej R, Sobesky J, et al. The choice of embedding media affects image quality, tissue  $R_2^*$ , and susceptibility behaviors in post-mortem brain MR microscopy at 7.0T: DUSEK et al. *Magn Reson Med* 2019; 81: 2688–701.
- Düzel E, Guitart-Masip M, Maass A, Hämmerer D, Betts MJ, Speck O, et al. Midbrain fMRI: applications, limitations and challenges. In: Uludag K, Ugurbil K, Berliner L, editors. *fMRI: From Nuclear Spins to Brain Functions*. Boston, MA: Springer US; 2015. p. 581–609
- Ehrenberg AJ, Nguy AK, Theofilas P, Dunlop S, Suemoto CK, Di Lorenzo Alho AT, et al. Quantifying the accretion of hyperphosphorylated tau in the locus coeruleus and dorsal raphe nucleus: the pathological building blocks of early Alzheimer's disease. *Neuropathol Appl Neurobiol* 2017; 43: 393–408.
- Ehrenberg AJ, Suemoto CK, de Paula França Resende E, Petersen C, Leite REP, Rodriguez RD, et al. Neuropathologic correlates of psychiatric symptoms in Alzheimer's disease. *J Alzheimers Dis* 2018; 66: 115–126.
- Engelen M, Vanna R, Bellei C, Zucca FA, Wakamatsu K, Monzani E, et al. Neuromelanins of human brain have soluble and insoluble components with dolichols attached to the melanic structure. *PLoS One* 2012; 7: e48490.
- Ennis M, Behbehani M, Shipley MT, van Bockstaele EJ, Aston-Jones G. Projections from the periaqueductal gray to the rostromedial pericoerulear region and nucleus locus coeruleus: Anatomic and physiologic studies. *J Comp Neurol* 1991; 306: 480–94.
- Enochs WS, Hyslop WB, Bennett HF, Brown III RD, Koenig SH, Swartz HM. Sources of the increased longitudinal relaxation rates observed in melanotic melanoma. An *in vitro* study of synthetic melanins. *Invest Radiol* 1989; 24: 794–804.
- Enochs WS, Petherick P, Bogdanova A, Mohr U, Weissleder R. Paramagnetic metal scavenging by melanin: MR imaging. *Radiology* 1997; 204: 417–23.
- Eser RA, Ehrenberg AJ, Petersen C, Dunlop S, Mejia MB, Suemoto CK, et al. Selective vulnerability of brainstem nuclei in distinct tauopathies: a postmortem study. *J Neuropathol Exp Neurol* 2018; 77: 149–61.
- Espay AJ, LeWitt PA, Kaufmann H. Norepinephrine deficiency in Parkinson's disease: the case for noradrenergic enhancement: norepinephrine deficiency in PD. *Mov Disord* 2014; 29: 1710–9.
- Finnema SJ, Nabulsi NB, Eid T, Detyniecki K, Lin S, Chen M-K, et al. Imaging synaptic density in the living human brain. *Sci Transl Med* 2016; 8: 348ra96.
- Forstmann BU, de Hollander G, van Maanen L, Alkemade A, Keuken MC. Towards a mechanistic understanding of the human subcortex. *Nat Rev Neurosci* 2017; 18: 57–65.
- Garcia-Lorenzo D, Longo-Dos Santos C, Ewencyk C, Leu-Semenescu S, Gallea C, Quattrocchi G, et al. The coeruleus/subcoeruleus complex in rapid eye movement sleep behaviour disorders in Parkinson's disease. *Brain* 2013; 136: 2120–9.
- German DC, Manaye KF, White CL, Woodward DJ, McIntire DD, Smith WK, et al. Disease-specific patterns of locus coeruleus cell loss. *Ann Neurol* 1992; 32: 667–76.
- German DC, Walker BS, Manaye K, Smith WK, Woodward DJ, North AJ. The human locus coeruleus: computer reconstruction of cellular distribution. *J Neurosci* 1988; 8: 1776–88.
- Giguère N, Burke Nanni S, Trudeau L-E. On cell loss and selective vulnerability of neuronal populations in Parkinson's disease. *Front Neurol* 2018; 9: 455. <https://www.frontiersin.org/article/10.3389/fneur.2018.00455/full> (21 February 2019, date last accessed).
- Haber SN, Knutson B. The reward circuit: linking primate anatomy and human imaging. *Neuropsychopharmacology* 2010; 35: 4–26.
- Hämmerer D, Callaghan MF, Hopkins A, Kosciessa J, Betts M, Cardenas-Blanco A, et al. Locus coeruleus integrity in old age is selectively related to memories linked with salient negative events. *Proc Natl Acad Sci* 2018: 201712268.
- Hämmerer D, Callaghan MF, Betts MJ, Cardenas-Blanco A, Kosciessa JQ, Weiskopf N, Dolan RJ, Düzel E. Multiparametric mapping of the Locus Coeruleus in ageing. Poster presented at Dementia MRI meeting, Cambridge; 2018a.
- Hansen AK, Knudsen K, Lillethorup TP, Landau AM, Parbo P, Fedorova T, et al. *In vivo* imaging of neuromelanin in Parkinson's disease using  $^{18}$ F-AV-1451 PET. *Brain* 2016; 139: 2039–49.
- Heneka MT. Locus coeruleus degeneration promotes Alzheimer pathogenesis in amyloid precursor protein 23 transgenic mice. *J Neurosci* 2006; 26: 1343–54.
- Heneka MT, Carson MJ, Khoury JE, Landreth GE, Brosseron F, Feinstein DL, et al. Neuroinflammation in Alzheimer's disease. *Lancet Neurol* 2015; 14: 388–405.
- Herrmann N, Lanctôt KL, Khan LR. The role of norepinephrine in the behavioral and psychological symptoms of dementia. *J Neuropsychiatry Clin Neurosci* 2004; 16: 261–76.
- Hoogendijk WJG, Feenstra MGP, Botterblom MHA, Gilhuis J, Sommer IEC, Kamphorst W, et al. Increased activity of surviving locus coeruleus neurons in Alzheimer's disease. *Ann Neurol* 1999; 45: 82–91.
- Irwin DJ, Bretschneider J, McMillan CT, Cooper F, Olm C, Arnold SE, et al. Deep clinical and neuropathological phenotyping of Pick disease: Deep Phenotype Pick Disease. *Ann Neurol* 2016; 79: 272–87.
- Jacobs HI, Becker A, Kwong K, d'Oleire Uquillas F, Sperling RA, Johnson KA. Locus coeruleus signal intensity is associated with entorhinal tau pathology at higher levels of amyloid burden. *Alzheimers Dement* 2018; 14: P509–10.
- Jacobs HIL, Müller-Ehrenberg L, Priovoulos N, Roebroek A. Curvilinear locus coeruleus functional connectivity trajectories over the adult lifespan: a 7T MRI study. *Neurobiol Aging* 2018; 69: 167–76.
- Jacobs HIL, Wiese S, van de Ven V, Gronenschild EHB, Verhey FRJ, Matthews PM. Relevance of parahippocampal-locus coeruleus connectivity to memory in early dementia. *Neurobiol Aging* 2015; 36: 618–26.
- Jardanhazi-Kurutz D, Kummer MP, Terwel D, Vogel K, Dyrks T, Thiele A, et al. Induced LC degeneration in APP/PS1 transgenic mice accelerates early cerebral amyloidosis and cognitive deficits. *Neurochem Int* 2010; 57: 375–82.
- Jessen F, Spottke A, Boecker H, Brosseron F, Buerger K, Catak C, et al. Design and first baseline data of the DZNE multicenter observational study on predementia Alzheimer's disease (DELCODE). *Alzheimers Res Ther* 2018; 10: 15.
- Kalinin S, Polak PE, Lin SX, Sakharkar AJ, Pandey SC, Feinstein DL. The noradrenaline precursor L-DOPS reduces pathology in a mouse model of Alzheimer's disease. *Neurobiol Aging* 2012; 33: 1651–63.
- Kalinin S, Polak PE, Madrigal JLM, Gavrilyuk V, Sharp A, Chauhan N, et al. Beta-amyloid-dependent expression of NOS2 in neurons: prevention by an  $\alpha$ 2-adrenergic antagonist. *Antioxid Redox Signal* 2006; 8: 873–83.
- Kelly SC, He B, Perez SE, Ginsberg SD, Mufson EJ, Counts SE. Locus coeruleus cellular and molecular pathology during the progression of Alzheimer's disease. *Acta Neuropathol Commun* 2017; 5: 8.
- Kempadoo KA, Mosharov EV, Choi SJ, Sulzer D, Kandel ER. Dopamine release from the locus coeruleus to the dorsal hippocampus promotes spatial learning and memory. *Proc Natl Acad Sci* 2016; 113: 14835–40.
- Keren NI, Lozar CT, Harris KC, Morgan PS, Eckert MA. *In vivo* mapping of the human locus coeruleus. *NeuroImage* 2009; 47: 1261–7.
- Keren NI, Taheri S, Vazey EM, Morgan PS, Granholm A-CE, Aston-Jones GS, et al. Histologic validation of locus coeruleus MRI contrast in post-mortem tissue. *NeuroImage* 2015; 113: 235–45.
- Knudsen K, Fedorova TD, Hansen AK, Sommerauer M, Otto M, Svendsen KB, et al. *In-vivo* staging of pathology in REM sleep

- behaviour disorder: a multimodality imaging case-control study. *Lancet Neurol* 2018; 17: 618–28.
- Krebs N, Langkammer C, Goessler W, Ropele S, Fazekas F, Yen K, et al. Assessment of trace elements in human brain using inductively coupled plasma mass spectrometry. *J Trace Elem Med Biol* 2014; 28: 1–7.
- Lancôt KL, Amatié J, Ancoli-Israel S, Arnold SE, Ballard C, Cohen-Mansfield J, et al. Neuropsychiatric signs and symptoms of Alzheimer's disease: new treatment paradigms. *Alzheimers Dement Transl Res Clin Interv* 2017; 3: 440–9.
- Langley J, Huddleston DE, Chen X, Sedlacik J, Zachariah N, Hu X. A multicontrast approach for comprehensive imaging of substantia nigra. *NeuroImage* 2015; 112: 7–13.
- Langley J, Huddleston DE, Liu CJ, Hu X, . Reproducibility of locus coeruleus and substantia nigra imaging with neuromelanin sensitive MRI. *Magn Reson Mater Physics, Biol Med* 2017; 30: 121–5.
- Lee CM, Jacobs HIL, Marquié M, Becker JA, Andrea NV, Jin DS, et al. 18F-Flortaucipir Binding in Choroid Plexus: Related to Race and Hippocampus Signal. *J Alzheimers Dis* 2018; 62: 1691–702.
- Liu KY, Acosta-Cabronero J, Cardenas-Blanco A, Loane C, Berry AJ, Betts MJ, et al. In vivo visualization of age-related differences in the locus coeruleus. *Neurobiol Aging* 2019; 74: 101–11.
- Liu KY, Marijatta F, Hämmerer D, Acosta-Cabronero J, Düzel E, Howard RJ. Magnetic resonance imaging of the human locus coeruleus: a systematic review. *Neurosci Biobehav Rev* 2017; 83: 325–55.
- Llorca-Torralba M, Borges G, Neto F, Mico JA, Berrocoso E. Noradrenergic locus coeruleus pathways in pain modulation. *Neuroscience* 2016; 338: 93–113.
- Louis ED, Faust PL, Vonsattel J-PG, Honig LS, Rajput A, Robinson CA, et al. Neuropathological changes in essential tremor: 33 cases compared with 21 controls. *Brain* 2007; 130: 3297–307.
- Lyness S. Neuron loss in key cholinergic and aminergic nuclei in Alzheimer disease: a meta-analysis. *Neurobiol Aging* 2003; 24: 1–23.
- Manaye KF, McIntire DD, Mann D, German DC. Locus coeruleus cell loss in the aging human brain: A non-random process. *J Comp Neurol* 1995; 358: 79–87.
- Mann DMA, Yates PO. Lipoprotein pigments—Their relationship to ageing in the human nervous system II. The melanin content of pigmented nerve cells. *Brain* 1974; 97: 489–498.
- Marquié M, Normandin MD, Vanderburg CR, Costantino IM, Bien EA, Rycyna LG, et al. Validating novel tau positron emission tomography tracer [F-18]-AV-1451 (T807) on postmortem brain tissue: validation of PET Tracer. *Ann Neurol* 2015; 78: 787–800.
- Mather M, Clewett D, Sakaki M, Harley CW. Norepinephrine ignites local hotspots of neuronal excitation: How arousal amplifies selectivity in perception and memory. *Behav Brain Sci* 2016; 39: e200.
- Mather M, Harley CW. The locus coeruleus: essential for maintaining cognitive function and the aging brain. *Trends Cogn Sci* 2016; 20: 214–26.
- Matsuura K, Maeda M, Yata K, Ichiba Y, Yamaguchi T, Kanamaru K, et al. Neuromelanin Magnetic resonance imaging in Parkinson's disease and multiple system atrophy. *Eur Neurol* 2013; 70: 70–77.
- McMillan PJ, White SS, Franklin A, Greenup JL, Leverenz JB, Raskind MA, et al. Differential response of the central noradrenergic nervous system to the loss of locus coeruleus neurons in Parkinson's disease and Alzheimer's disease. *Brain Res* 2011; 1373: 240–52.
- Moises HC, Waterhouse BD, Woodward DJ. Locus coeruleus stimulation potentiates Purkinje cell responses to afferent input: The climbing fiber system. *Brain Res* 1981; 222: 43–64.
- Nakane T, Nishihashi T, Kawai H, Naganawa S. Visualization of neuromelanin in the substantia nigra and locus ceruleus at 1.5 T Using a 3D-gradient echo sequence with magnetization transfer contrast. *Magn Reson Med Sci* 2008; 7: 205–10.
- O'Donnell J, Ding F, Nedergaard M. Distinct functional states of astrocytes during sleep and wakefulness: is norepinephrine the master regulator? *Curr Sleep Med Rep* 2015; 1: 1–8.
- Ohm TG, Busch C, Bohl J. Unbiased estimation of neuronal numbers in the human nucleus coeruleus during aging. *Neurobiol Aging* 1997; 18: 393–9.
- Palmer AM, Wilcock GK, Esiri MM, Francis PT, Bowen DM. Monoaminergic innervation of the frontal and temporal lobes in Alzheimer's disease. *Brain Res* 1987; 401: 231–8.
- Palmqvist S, Schöll M, Strandberg O, Mattsson N, Stomrud E, Zetterberg H, et al. Earliest accumulation of  $\beta$ -amyloid occurs within the default-mode network and concurrently affects brain connectivity. *Nat Commun* 2017; 8. <http://www.nature.com/articles/s41467-017-01150-x> (21 February 2019, date last accessed).
- Passamonti L, Lansdall C, Rowe J. The neuroanatomical and neurochemical basis of apathy and impulsivity in frontotemporal lobar degeneration. *Curr Opin Behav Sci* 2018; 22: 14–20.
- Pietrzak RH, Gallezot J-D, Ding Y-S, Henry S, Potenza MN, Southwick SM, et al. Association of posttraumatic stress disorder with reduced in vivo norepinephrine transporter availability in the locus coeruleus. *JAMA Psychiatry* 2013; 70: 1199.
- Priovoulos N, Jacobs HIL, Ivanov D, Uludag K, Verhey FRJ, Poser BA. High-resolution in vivo imaging of human locus coeruleus by magnetization transfer MRI at 3 T and 7 T. *NeuroImage* 2018; 168: 427–36.
- Robbins TW. Cortical noradrenaline, attention and arousal1. *Psychol Med* 1984; 14: 13.
- Robertson IH. A noradrenergic theory of cognitive reserve: implications for Alzheimer's disease. *Neurobiol Aging* 2013; 34: 298–308.
- Rorabaugh JM, Chalermphanupap T, Botz-Zapp CA, Fu VM, Lembeck NA, Cohen RM, et al. Chemogenetic locus coeruleus activation restores reversal learning in a rat model of Alzheimer's disease. *Brain* 2017; 140: 3023–38.
- Roy B, Wang Q, Palkovits M, Faludi G, Dwivedi Y. Altered miRNA expression network in locus coeruleus of depressed suicide subjects. *Sci Rep* 2017; 7: 4387.
- Sara SJ. The locus coeruleus and noradrenergic modulation of cognition. *Nat Rev Neurosci* 2009; 10: 211–23.
- Sasaki M, Shibata E, Tohyama K, Takahashi J, Otsuka K, Tsuchiya K, et al. Neuromelanin magnetic resonance imaging of locus ceruleus and substantia nigra in Parkinson's disease. *Neuroreport* 2006; 17: 1215–8.
- Seidel K, Mahlke J, Siswanto S, Krüger R, Heinsen H, Auburger G, et al. The Brainstem pathologies of Parkinson's Disease and dementia with lewy bodies: the brainstem in iPD and DLB. *Brain Pathol* 2015; 25: 121–35.
- Sharma Y, Xu T, Graf WM, Fobbs A, Sherwood CC, Hof PR, et al. Comparative anatomy of the locus coeruleus in humans and nonhuman primates. *J Comp Neurol* 2010; 518: 963–71.
- Shibata E, Sasaki M, Tohyama K, Kanbara Y, Otsuka K, Ehara S, et al. Age-related changes in locus ceruleus on neuromelanin magnetic resonance imaging at 3 tesla. *Magn Reson Med Sci* 2006; 5: 197–200.
- Shima T, Sarna T, Swartz HM, Stroppolo A, Gerbasi R, Zecca L. Binding of iron to neuromelanin of human substantia nigra and synthetic melanin: an electron paramagnetic resonance spectroscopy study. *Free Radic Biol Med* 1997; 23: 110–9.
- Sommerauer M, Fedorova TD, Hansen AK, Knudsen K, Otto M, Jeppesen J, et al. Evaluation of the noradrenergic system in Parkinson's disease: an 11 C-MeNER PET and neuromelanin MRI study. *Brain* 2018; 141: 496–504.
- Stankovic I, Krismer F, Jesic A, Antonini A, Benke T, Brown RG, et al. Cognitive impairment in multiple system atrophy: a position statement by the neuropsychology task force of the MDS multiple system atrophy (MODMSA) study group: COGNITIVE IMPAIRMENT IN MSA. *Mov Disord* 2014; 29: 857–67.
- Stein TD, Alvarez VE, McKee AC. Chronic traumatic encephalopathy: a spectrum of neuropathological changes following repetitive brain trauma in athletes and military personnel. *Alzheimers Res Ther* 2014; 6: 4.

- Stern RA, Daneshvar DH. Clinical presentation of chronic traumatic encephalopathy. *Neurology* 2013; 81: 1122–9.
- Sterpenich V, D'Argembeau A, Desseilles M, Baetens E, Albouy G, Vandewalle G, et al. The locus ceruleus is involved in the successful retrieval of emotional memories in humans. *J Neurosci* 2006; 26: 7416–23.
- Stratmann K, Heinsen H, Korf H-W, Del Turco D, Ghebremedhin E, Seidel K, et al. Precortical phase of Alzheimer's Disease (AD)-related tau cytoskeletal pathology: precortical phases of AD. *Brain Pathol* 2016; 26: 371–86.
- Sulzer D, Cassidy C, Horga G, Kang UJ, Fahn S, Casella L, et al. Neuromelanin detection by magnetic resonance imaging (MRI) and its promise as a biomarker for Parkinson's disease. *NPJ Park Dis* 2018; 4: 11.
- Tabrez S, R. Jabir N, Shakil S, H. Greig N, Alam Q, M. Abuzenadah A, et al. A synopsis on the role of tyrosine hydroxylase in Parkinson's disease. *CNS Neurol Disord - Drug Targets* 2012; 11: 395–409.
- Takeuchi T, Duszkiwicz AJ, Sonneborn A, Spooner PA, Yamasaki M, Watanabe M, et al. Locus coeruleus and dopaminergic consolidation of everyday memory. *Nature* 2016; 537: 357–62.
- Taylor BK, Westlund KN. The noradrenergic locus coeruleus as a chronic pain generator: Is the LC a Neuropathic Pain Generator? *J Neurosci Res* 2017; 95: 1336–46.
- Terry RD, Masliah E, Salmon DP, Butters N, DeTeresa R, Hill R, et al. Physical basis of cognitive alterations in Alzheimer's disease: synapse loss is the major correlate of cognitive impairment. *Ann Neurol* 1991; 30: 572–80.
- Theofilas P, Ehrenberg AJ, Dunlop S, Di Lorenzo Alho AT, Nguy A, Leite REP, et al. Locus coeruleus volume and cell population changes during Alzheimer's disease progression: a stereological study in human postmortem brains with potential implication for early-stage biomarker discovery. *Alzheimers Dement* 2017; 13: 236–46.
- Tona K-D, Keuken MC, de Rover M, Lakke E, Forstmann BU, Nieuwenhuis S, et al. In vivo visualization of the locus coeruleus in humans: quantifying the test–retest reliability. *Brain Struct Funct* 2017; 222: 4203–17.
- Trujillo P, Summers PE, Ferrari E, Zucca FA, Sturini M, Mainardi LT, et al. Contrast mechanisms associated with neuromelanin-MRI: Neuromelanin-MRI Contrast. *Magn Reson Med* 2017; 78: 1790–800.
- Van Bockstaele EJ, Colago EEO, Valentino RJ. Amygdaloid corticotropin-releasing factor targets locus coeruleus dendrites: substrate for the co-ordination of emotional and cognitive limbs of the stress response. *J Neuroendocrinol* 2006; 10: 743–58.
- Wakamatsu K, Tabuchi K, Ojika M, Zucca FA, Zecca L, Ito S. Norepinephrine and its metabolites are involved in the synthesis of neuromelanin derived from the locus coeruleus. *J Neurochem* 2015; 135: 768–76.
- Walsh RR, Krismer F, Galpern WR, Wenning GK, Low PA, Halliday G, et al. Recommendations of the global multiple system atrophy research roadmap meeting. *Neurology* 2018; 90: 74–82.
- Ward RJ, Zucca FA, Duyn JH, Crichton RR, Zecca L. The role of iron in brain ageing and neurodegenerative disorders. *Lancet Neurol* 2014; 13: 1045–60.
- Watanabe T, Tan Z, Wang X, Martinez-Hernandez A, Frahm J. Magnetic resonance imaging of noradrenergic neurons. *Brain Struct Funct* 2019; 244: 1609–25.
- Weinshenker D. Long road to ruin: noradrenergic dysfunction in neurodegenerative disease. *Trends Neurosci* 2018; 41: 211–23.
- Weiskopf N, Suckling J, Williams G, Correia MM, Inkster B, Tait R, et al. Quantitative multi-parameter mapping of R1, PD\*, MT, and R2\* at 3T: a multi-center validation. *Front Neurosci* 2013; 7. <http://journal.frontiersin.org/article/10.3389/fnins.2013.00095/abstract> (30 October 2018, date last accessed).
- Wilson RS, Nag S, Boyle PA, Hibel LP, Yu L, Buchman AS, et al. Neural reserve, neuronal density in the locus coeruleus, and cognitive decline. *Neurology* 2013; 80: 1202–8.
- Ye Z, Altena E, Nombela C, Housden CR, Maxwell H, Rittman T, et al. Improving response inhibition in Parkinson's disease with atomoxetine. *Biol Psychiatry* 2015; 77: 740–8.
- Zarow C, Lyness SA, Mortimer JA, Chui HC. Neuronal loss is greater in the locus coeruleus than nucleus basalis and substantia nigra in Alzheimer and Parkinson diseases. *Arch Neurol* 2003; 60: 337.
- Zecca L, Stroppolo A, Gatti A, Tampellini D, Toscani M, Gallorini M, et al. The role of iron and copper molecules in the neuronal vulnerability of locus coeruleus and substantia nigra during aging. *Proc Natl Acad Sci USA* 2004; 101: 9843–8.
- Zucca FA, Bellei C, Giannelli S, Terreni MR, Gallorini M, Rizzio E, et al. Neuromelanin and iron in human locus coeruleus and substantia nigra during aging: consequences for neuronal vulnerability. *J Neural Transm* 2006; 113: 757–67.
- Zucca FA, Segura-Aguilar J, Ferrari E, Muñoz P, Paris I, Sulzer D, et al. Interactions of iron, dopamine and neuromelanin pathways in brain aging and Parkinson's disease. *Prog Neurobiol* 2017; 155: 96–119.
- Zucca FA, Vanna R, Cupaioli FA, Bellei C, De Palma A, Di Silvestre D, et al. Neuromelanin organelles are specialized autolysosomes that accumulate undegraded proteins and lipids in aging human brain and are likely involved in Parkinson's disease. *NPJ Park Dis* 2018; 4: 17.